

# Biosynthesis of TiO<sub>2</sub> and ZnO nanoparticles by *Halomonas elongata* IBRC-M 10214 in different conditions of medium

Mojtaba Taran, Maryam Rad, Mehran Alavi\*

Microbiology Laboratory, Department of Biology, Faculty of Science, Razi University, Kermanshah, Iran

## Article Info



### Article Type:

Original Article

### Article History:

Received: 11 June 2017

Revised: 2 Dec. 2017

Accepted: 3 Dec. 2017

ePublished: 27 Dec. 2017

### Keywords:

Antibacterial activities,  
 Biosynthesis,  
*Halomonas elongata*  
 IBRC-M 10214,  
 Metal nanoparticles,  
 Optimization,  
 Taguchi method

## Abstract

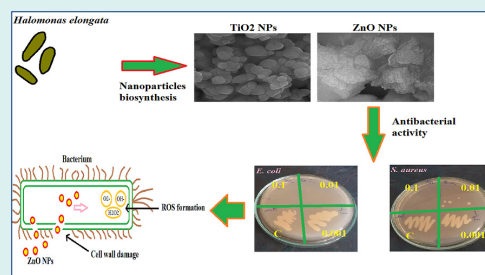
**Introduction:** In the recent years, green synthesis is a novel method without some disadvantages of physical and chemical methods. In this approach, bacteria, archaeobacteria, fungi, and plants may be applied without utilizing toxic and expensive materials for metal nanoparticles (MNPs) preparation.

**Methods:** In this study, we used Taguchi method to obtain optimum conditions in titanium dioxide and zinc oxide nanoparticle (NPs) biosynthesis by *Halomonas elongata* IBRC-M 10214.

Design and analysis of Taguchi experiments (an orthogonal assay and analysis of variance [ANOVA]) carried out by the Qualitek-4 software. Effects of TiO(OH)<sub>2</sub>, incubation temperature, and culturing time for synthesis of TiO<sub>2</sub> NPs as well as ZnCl<sub>2</sub> concentration, glucose concentration, and incubation temperature for the preparation of ZnO NPs were evaluated as the controllable factors with 3 levels. Characterization of TiO<sub>2</sub> and ZnO NPs were determined by UV-Vis spectroscopy, X-ray diffraction (XRD), Fourier transform infrared spectroscopy (FT-IR), scanning electron microscopy (SEM), and dynamic light scattering (DLS) analysis. Also, the antimicrobial properties of these NPs were investigated based on agar diffusion assay of NPs dispersed in batch cultures using *Escherichia coli* ATCC 25922 and *Staphylococcus aureus* ATCC 43300 as multidrug-resistant (MDR) bacteria.

**Results:** It was evaluated that TiO<sub>2</sub> and ZnO NPs had respectively average diameter sizes of 104.63±27.75 and 18.11±8.93 nm with spherical shapes. In contrast to the TiO<sub>2</sub> NPs without antibacterial activity, the ZnO NPs had antibacterial effects at 0.1 and 0.01 M of (ZnCl<sub>2</sub>).

**Conclusion:** The ZnO NPs have the antibacterial effect that can be operative in the medicinal aspect for fighting against prominent MDR bacteria such as *E. coli* ATCC 25922 and *S. aureus* ATCC 43300. In total, this study presents a simple method in the biosynthesis of TiO<sub>2</sub> and ZnO NPs with the low expense, eco-friendly, and high productivity properties.



## Introduction

The insensitivity of microorganisms to antimicrobial agents is named as multidrug-resistance (MDR), which is increasing dramatically.<sup>1</sup> MDR microorganisms including bacteria, parasites, viruses and fungi use various strategies to neutralize the effect of antimicrobial drugs.<sup>2</sup> Among microorganisms, the MDR phenomenon is prominent in bacteria such as *Escherichia coli*, *Staphylococcus aureus*, *Klebsiella pneumoniae*, *Streptococcus pneumoniae* and *Neisseria gonorrhoeae*.<sup>3</sup> The resistance of these bacteria to antibiotics is resulted from the achievement of specific properties related to the membrane structures and enzymes generation.<sup>4</sup> Recently, nanotechnology introduces a new

alternative to overcome this problem.<sup>5</sup> The synthesis of nanoparticles (NPs) ranging from approximately 1-100 nm with various physicochemical properties is an important area in nanotechnology investigations.<sup>6</sup> These properties have been enabled NPs applications in a wide range of science and technology specifically nanobiotechnology.<sup>7</sup> Due to different applications of nanobiotechnology, this scientific field has been received worldwide attention chiefly among researchers.<sup>8</sup> In this case, metallic NPs (MNPs) such as TiO<sub>2</sub>, Ag, Au, ZnO, MgO and CuO NPs can be utilized in biological and biomedicine systems.<sup>9,10</sup>

There are several methods for synthesis of MNPs such as physical and chemical methods.<sup>11</sup> The most

\*Corresponding author: Mehran Alavi, Email: mehranbio83@gmail.com



physical techniques are laser ablation and evaporation-condensation.<sup>12</sup> The physical synthesis of MNPs by a tube furnace at normal pressure has some disadvantages, including the need for the large space in this type of furnace and high amount of energy. In addition, time-consuming of physical methods is another disadvantage. In chemical methods, the most common approach is using organic and inorganic reducing agents (such as sodium borohydride [NaBH<sub>4</sub>], polyol, ascorbate, and sodium citrate) as chemical reduction method for MNPs synthesis.<sup>13</sup> In chemical methods, reducing agents can reduce metal ions which resulted in the formation of MNPs.<sup>14</sup> Disadvantages of these methods are using toxic and expensive chemicals in the synthesis process.<sup>15</sup>

In recent years, green synthesis is a novel method without some disadvantages of physical and chemical methods.<sup>16</sup> In this approach, bacteria, archaeobacteria, fungi, and plants may be applied without utilizing toxic and expensive materials for MNPs preparation.<sup>17-20</sup> In this case, size distribution and morphologies of the MNPs can be controlled by changing reaction conditions such as pH, temperature, culturing time, metal salts concentration, electron donor of reaction media such as fructose and glucose and etc. Therefore, based on these advantages of MNPs green synthesis, in this study, the selected strain *Halomonas elongata* IBRC-M 10214 was applied as to TiO<sub>2</sub> and ZnO NPs. UV-visible spectroscopy, X-ray diffraction (XRD), Fourier Transform Infra-Red spectroscopy (FT-IR), scanning electron microscopy (SEM) and dynamic light scattering (DLS) techniques were applied for the characterization of NPs. Also, antibacterial effects of the final reaction were evaluated on two pathogenesis bacteria strain with multidrug-resistant property, *Escherichia coli* ATCC 25922 and *Staphylococcus aureus* ATCC 43300.

## Materials and Methods

### Taguchi methodology experimental design

The robust design of Taguchi was used to reduce the cost and improvement quality of experiment. Due to optimization of experimental conditions, all the combination experiments using the assigned parameter values were conducted. The Qualitek-4 software was used to design and analyze Taguchi experiments as a statistical

method.<sup>21,22</sup> Tables 1 and 2 demonstrate 3 controllable factors with 3 levels (TiO(OH)<sub>2</sub> concentration, incubation temperature, culturing time for TiO<sub>2</sub> NPs and ZnCl<sub>2</sub> concentration, glucose concentration and incubation temperature for ZnO NPs) in the design of the experiment.

### Materials

Metatitanic acid (TiO(OH)<sub>2</sub>) and zinc chloride (ZnCl<sub>2</sub>) were purchased from Sigma-Aldrich (St. Louis, USA) and applied respectively for TiO<sub>2</sub> and ZnO NPs biosynthesis without any further purification. Also, for antibacterial activity measurement, Muller Hinton Broth (MHB) and Muller Hinton Agar (MHA) were procured from Sigma-Aldrich (St. Louis, USA).

### TiO<sub>2</sub> and ZnO NPs biosynthesis and preparation of supernatant

*Halomonas elongata* IBRC-M 10214 with property of metal resistance was obtained from bacterial archive of Razi University of Kermanshah and cultivated in the basal medium contains (g/L) glucose, 10; MgSO<sub>4</sub>, 1.4; NaCl, 150; NH<sub>4</sub>Cl, 2.3; K<sub>2</sub>HPO<sub>4</sub>, 0.6; FeSO<sub>4</sub>, 0.001 and 10% (V/V).<sup>23</sup> The inoculum was transferred into 100 mL Erlenmeyer flasks and incubated in a shaker at 37°C for one week. According to the details following the experiment design, the growth medium was supplemented with various nutrients compositions by varying glucose (Table 2). The amount of 1.5 mL from each Erlenmeyer flask was centrifuged at 10000 rpm for 5 minutes. Afterward, 1 mL of the supernatant was poured test tube followed by treating with different concentrations of TiO(OH)<sub>2</sub> and ZnCl<sub>2</sub> (Tables 1 and 2). In the end, the resulted solution was placed at 28°C in a shaking incubator with the set at 120 rpm.<sup>24</sup>

### Nanoparticles characterization

The intensity of absorption peaks and peak absorbance of NPs was examined by UV-Vis spectrophotometer (Tomas, UV 331) from 200 to 800 nm. FT-IR measurements were carried out by spectrophotometer (Bruker, ALPHA, Bremen, Germany). The prepared annealed samples were analyzed by XRD analysis, SEM due to the evaluation of structure, morphology and elemental composition

**Table 1.** Parameters and their levels in biosynthesis TiO<sub>2</sub> NPs

Symbol	Parameters	Unit	Level 1	Level 2	Level 3
A	TiO(OH) <sub>2</sub> concentration	Molar (M)	0.1	0.01	0.001
B	Incubation temperature	°C	25	30	37
C	Culturing time	Hour	48	72	96

**Table 2.** Parameters and their levels in biosynthesis of ZnO NPs

Symbol	Parameters	Unit	Level 1	Level 2	Level 3
A	ZnCl <sub>2</sub> concentration	Molar (M)	0.1	0.01	0.001
B	Glucose concentration	Molar (M)	0.05	0.07	1
C	Incubation temperature	°C	25	30	37

of NPs. DLS analysis was applied to determine the zeta average diameter and polydispersity index (PDI) of NPs using Zetasizer (Nano-ZS, Malvern, UK). The crystallographic study was carried out using EQUINOX 3000, diffractometer in the scanning range of 20°-70° (2θ) using Cu Kα radiations of wavelength 1.5406 Å. field emission scanning electron microscope (FESEM) (XL30, Philips, Eindhoven, The Netherlands) was applied to determine the morphology of the NPs and the elemental analysis.

### Bacteria preparation

Reprehensive multidrug-resistant bacteria of gram-negative (*E. coli* ATCC 25922) and gram-positive (*S. aureus* ATCC 43300) were applied to determine the antimicrobial activity of ZnO and TiO<sub>2</sub> NPs. These strains were obtained from the bacterial archive of microbiology laboratory, Razi University of Kermanshah (Kermanshah, Iran). In order to follow below evaluation, bacterial strains were maintained on the nutrient agar slants at 4°C.

### Antibacterial activity

Agar diffusion assay with minor modification was applied to indicate antibacterial activity of NPs.<sup>25</sup> Overnight Muller Hinton Broth (MHB) cultures of pathogenic bacteria *E. coli* ATCC 25922 and *S. aureus* ATCC 43300 were prepared freshly for each assay. These cultures were mixed with sterile physiological saline and turbidity was indicated by adding physiological saline until obtaining of a 0.5 McFarland turbidity standard ( $1.5 \times 10^8$  CFU/mL). Petri plates were prepared with 20 mL of sterile Muller Hinton Agar (MHA) and 24 hours prepared test cultures of inoculums were swabbed on the surface of the solidified media. After drying of media for 10 minutes biosynthesized TiO<sub>2</sub> and ZnO NPs at the different concentrations of TiO(OH)<sub>2</sub> and ZnCl<sub>2</sub> (0.1, 0.01 and 0.001 M), were added to bacteria medium.<sup>26,27</sup> Afterward, different concentrations were compared with each other.

## Results

### Taguchi method

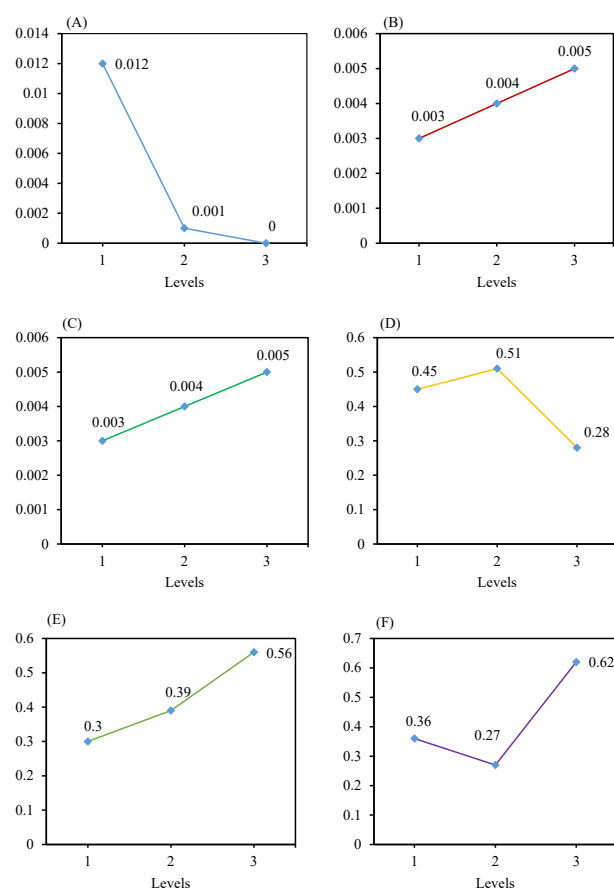
As shown in Table 1, 3 levels of TiO(OH)<sub>2</sub> concentration, incubation temperature and culturing time were respectively (0.1, 0.01 and 0.001 M), (25, 30 and 37°C) and (48, 72 and 96 hours). Also, parameters and their levels (incubation time, ZnCl<sub>2</sub> and glucose concentrations) in the biosynthesis of ZnO NPs were illustrated in Table 2. Based on Taguchi design method, nine experiments were carried out as an orthogonal array (Table S1 and S2).

Table S3 demonstrates effects of 3 different factors on the TiO<sub>2</sub> NPs biosynthesis by *H. elongata* IBRC-M 10214. As illustrated in this table, TiO(OH)<sub>2</sub> concentration in level 1 (0.012), incubation temperature in level 3 (0.005) and culturing time in level 3 (0.005) had a higher effect on the TiO<sub>2</sub> NPs biosynthesis. Similarly, Taguchi results of the average effect of 3 parameters at TiO<sub>2</sub> and ZnO NPs biosynthesis are presented in Fig. 1.

The effects of 3 different factors by *H. elongata* IBRC-M 10214 are shown in Table S4. As shown in this table, ZnCl<sub>2</sub> concentration in level 2 (0.514), incubation temperature in level 3 (0.562) and culturing time in level 3 (0.617) had a higher effect on the ZnO NPs biosynthesis. Also, Fig. 1 illustrates the average effect of 3 factors on the ZnO NPs biosynthesis.

Effective factors in TiO<sub>2</sub> and ZnO NPs biosynthesis by *H. elongata* IBRC-M 10214 are shown by variance analysis (ANOVA) (Table S5 and S6). Final column determines effect percentage of each factor which major factors for TiO<sub>2</sub> and ZnO NPs biosynthesis are respectively TiO(OH)<sub>2</sub> concentration with a value of 44.88% and culturing time by the value of 35.736%. Therefore, this result illustrates the higher importance of TiO(OH)<sub>2</sub> concentration and culturing time parameters than other parameters respectively in TiO<sub>2</sub> and ZnO NPs biosynthesis by *H. elongata* IBRC-M 10214.

Also, in Table S7 and Table 3, there are optimum conditions for biosynthesis of TiO<sub>2</sub> NPs and ZnO NPs affected by 3 factors. Expected results at optimum condition were values of 0.013% and 0.861% that are respectively suitable results for TiO<sub>2</sub> and ZnO NPs biosynthesis by this bacterium.



**Fig. 1.** Taguchi results of average effect of 3 parameters. Taguchi results of average effect of TiO(OH)<sub>2</sub> concentration (A), incubation temperature (B), culturing time (C), ZnCl<sub>2</sub> concentration (D), glucose concentration (E) and incubation temperature (F).

**Table 3.** Optimum conditions of ZnO NPs biosynthesis by bacterium

Factors	Level	Contribution
A	2	0.098
B	3	0.146
C	3	0.201
Total contribution from all factors	-	0.445
Current grand average of performance	-	0.416
Expected result at optimum condition	-	0.861

### UV-Visible spectroscopy

When cell-free supernatant of *Halomonas elongata* IBRC-M 10214 was added to  $\text{TiO}(\text{OH})_2$  and  $\text{ZnCl}_2$  solution and incubated for 3 times of incubation (48, 72, 96), the mixture's color reaction altered respectively from white to milky and colorless to opalescent color (Fig. 2A-B). In this study, reduction of titanium ions present in the aqueous solution of  $\text{TiO}(\text{OH})_2$  during the reduction by the ingredients of *Halomonas elongata* IBRC-M 10214 has been illustrated with the UV-Vis spectroscopy ranging from 200 to 800 nm. Fig. 3 illustrates the UV-Vis absorption spectra of biosynthesized  $\text{TiO}_2$  NPs in different concentrations of the  $\text{TiO}(\text{OH})_2$  solution (0.1, 0.01 and 0.001 M). A strong broad absorption band has been located between 300 and 400 nm for  $\text{TiO}_2$  NPs prepared by this bacterium.<sup>28,29</sup> The absorbance in this range was higher in 0.1 M of  $\text{TiO}(\text{OH})_2$  concentration. As illustrated in Fig. 3, ZnO NPs shows higher absorption peak at a wavelength of 267 nm which can be attributed to the intrinsic band-gap absorption of ZnO NPs. This property is resultant of the electron transition from the valence band to the conduction band.<sup>30</sup> Similar to  $\text{TiO}_2$  NPs, the higher absorption peak of ZnO NPs was in 0.1 M concentration of  $\text{ZnCl}_2$ .

### XRD analysis

Fig. 4 shows the XRD pattern of titanium dioxide NPs synthesized by *H. elongata* IBRC-M 10214. All the diffraction peaks (101), (004), (200) and (211) are indicated well to anatase crystalline phase of  $\text{TiO}_2$  NPs compared with JCPDs file No. (21-1275).<sup>31,32</sup> The determined characteristics  $2\theta$  values and (hkl) planes are 24.43 (101), 39.23 (004), 49.11 (200), 55.41 (105) and 57.12 (211) attributed to purity crystalline form of NPs.<sup>33</sup> In the case of ZnO NPs, all diffraction peaks (100), (002),

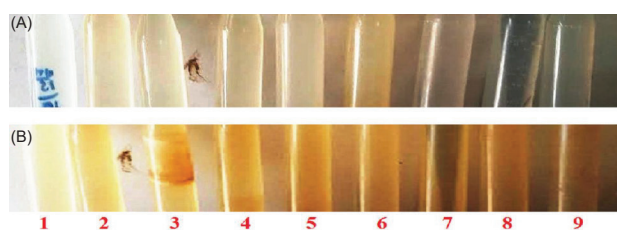


**Fig. 2.** Colour changes of solution. Changes of reaction mixture's colour from colourless to opalescent colour related to ZnO NPs formation (A) and white to milky related to  $\text{TiO}_2$  NPs formation (B) after supernatant addition (left to right).

(101), (110), (103), (112) and (202) are indicated ZnO hexagonal phase by comparison with JCPDS card No.89-7102.<sup>30,34</sup> The evaluated characteristics  $2\theta$  values and (hkl) planes are 31.21 (100), 35.44 (002), 37.15 (101), 57.56 (110), 65.25 (103), 68.33 (112) and 76.66 (202) attributed to purity crystalline form of NPs. Also, the mean size of two types of NPs was estimated with the Debye-Scherrer's equation:

$$\tau = \frac{K\lambda}{\beta \cos \theta}$$

Where,  $\tau$  is the mean diameter of the nanocrystal domains,  $k$  is a dimensionless shape factor with a value of about 0.9,  $\lambda$  is the wavelength of XRD source,  $\beta$  is the width at half the maximum intensity (FWHM) and  $\theta$  is the Bragg angle (in degree). The leaf extract prepared  $\text{TiO}_2$  NPs and ZnO NPs were quite polydisperse calculated respectively average size of 46.31 and 23.12 nm (Fig. 4).

### FT-IR spectrum analysis

FT-IR was applied to evaluate the possible molecular, responsible for the metal precursors reduction and  $\text{TiO}_2$  capping.<sup>35</sup> In the case of  $\text{TiO}_2$  NPs, as illustrated in Fig.

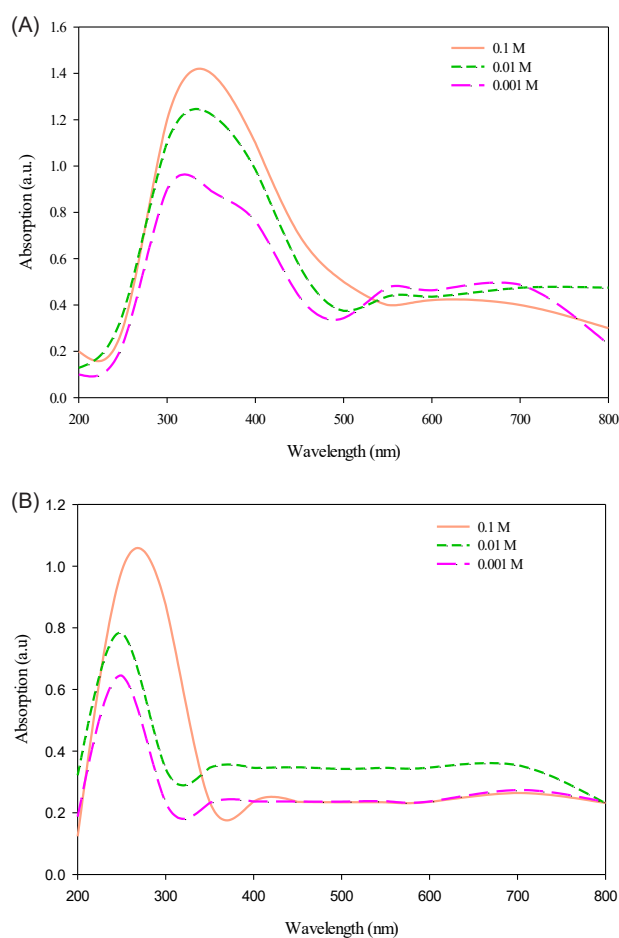


**Fig. 3.** UV-Visible spectroscopy. UV-Vis spectra of  $\text{TiO}_2$  (A) and ZnO (B) NPs biosynthesized by *Halomonas elongata* IBRC-M 10214 at different concentrations of  $\text{TiO}(\text{OH})_2$  and  $\text{ZnCl}_2$  solution: 0.001, 0.01, and 0.1 M.



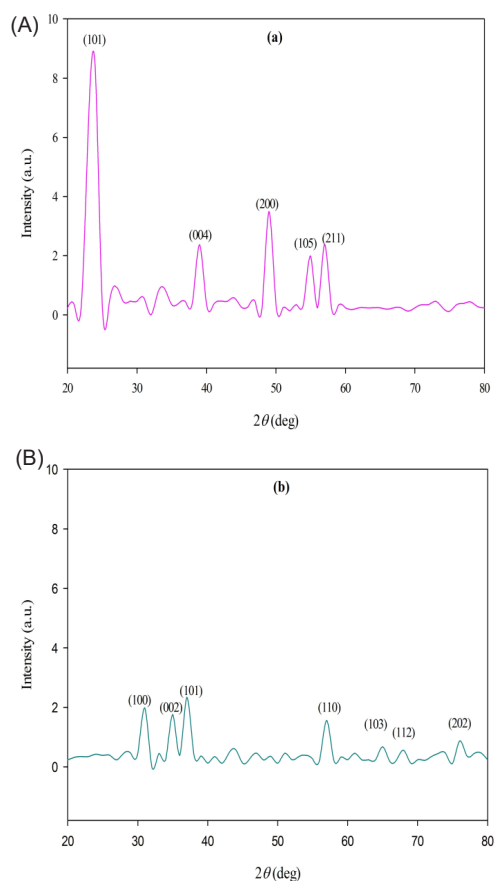


**Fig. 4.** XRD analysis. XRD patterns of titanium dioxide (A) and zinc oxide (B) NPs synthesized by *Halomonas elongata* IBRC-M 10214.

5, different bands at 3447.16, 2109.80, 1631.31, 1048.67, 773.50, 628.93, 561.33 and 416.07  $\text{cm}^{-1}$  are attributed respectively to O-H (alcohol),  $\text{-C}\equiv\text{C-}$  (alkyne) and  $\text{C}=\text{C}$  (alkene) stretching bonds.<sup>32</sup> Also, bands at 1048.67, 773.50, 628.93, 561.33 and 416.07  $\text{cm}^{-1}$  are assigned to alkyl halide groups including respectively C-F, C-Cl, C-Cl, C-Br, and C-I. The peaks at 989.98  $\text{cm}^{-1}$  correspond to  $=\text{C-H}$  bending strong bond.<sup>36,37</sup> FT-IR results show attribution of different functional groups in *H. elongata* IBRC-M 10214 including alcohol, alkyne, alkene and alkyl halide for TiO<sub>2</sub> NPs formation.<sup>36-38</sup> Also, the absorption band at around 3447.16  $\text{cm}^{-1}$  indicates to Ti-O stretches of TiO<sub>2</sub> NPs.<sup>39,40</sup>

#### SEM images and DLS analysis

The high density of TiO<sub>2</sub> and ZnO NPs are demonstrated in the solid phase by SEM analysis. Fig. 6 shows ZnO NPs had a higher density than TiO<sub>2</sub> NPs. Average diameter sizes for TiO<sub>2</sub> and ZnO NPs were respectively  $104.63\pm 27.75$  and  $18.11\pm 8.93$  nm. In the case of NPs morphology, TiO<sub>2</sub> NPs had a spherical shape, but ZnO NPs showed multiform shapes. Therefore, this analysis indicated smaller diameter and uniform shape of NPs. The DLS pattern indicated that TiO<sub>2</sub> and ZnO NPs biosynthesized by this bacterium have respectively the Zeta average diameter of  $98\pm 3.5$  and  $26\pm 2.4$  nm with PDI of 0.45 and 0.39. Besides, the DLS analysis of TiO<sub>2</sub> and ZnO NPs compared to SEM images

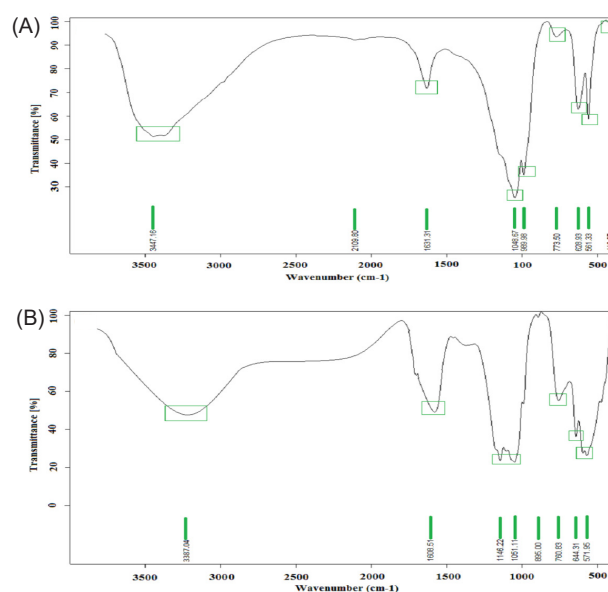


**Fig. 5.** FT-IR spectrum analysis. FT-IR spectrum of biosynthesized TiO<sub>2</sub> (a) and ZnO (b) NPs by *Halomonas elongata* IBRC-M 10214.

analysis showed slightly smaller and bigger particles size. *Bacillus subtilis* and *Bacillus mycoides* respectively show average diameter size in the range of 10-30 nm (spherical shape) and 40-60 nm (spherical shape) at room temperature condition.<sup>41,42</sup> Further, the green synthesis of ZnO NPs by *Aeromonas hydrophila* bacterium had NPs diameter in the range of 57-75 nm with a spherical shape.<sup>43</sup>

#### Antibacterial activity

The antibacterial activity of ZnO NPs was determined against 2 multidrug resistance bacteria *E. coli* ATCC 25922 and *S. aureus* ATCC 43300 by agar diffusion assay. A lack of the growth of bacteria was observed as confirmation of antibacterial activity after incubation of the plates (Fig. 7). Biosynthesized ZnO NPs had antibacterial effect only at 0.1 and 0.01 M of (ZnCl<sub>2</sub>). In return, TiO<sub>2</sub> NPs had not any antibacterial activity. Antibacterial and antifungal activities of biosynthesized ZnO NPs by *Aeromonas hydrophila* bacterium against *Pseudomonas aeruginosa* and *Aspergillus flavus* species was investigated by a previous study.<sup>43</sup> Agar well diffusion assay for *Citrobacter freundii*, *Proteus mirabilis*, *S. aureus*, and *Serratia marcescens* showed sensitivity to ZnO NPs as values of 19.16, 27.24, 26.23, and 24.21 mm respectively.<sup>44</sup> Also, green synthesized ZnO NPs with 29.79 nm had antimicrobial activities against *E. coli*, *S. aureus*, *Salmonella paratyphi*, and *Vibrio cholera*.<sup>45</sup>

The antibacterial activity of metal oxide NPs against gram-negative and gram-positive bacteria have surveyed by several investigators.<sup>46-49</sup> Efficiency of antibacterial agents may be related to the cell wall property of bacteria. Gram-negative bacteria are composed of 2 cell membranes (outer and plasma membrane) with a thin layer of peptidoglycan (about 8 nm) than gram-positive by thick cell wall (about 80 nm).<sup>50</sup> Therefore, NPs with a size of 8-80 nm can penetrate the cell wall of bacteria.<sup>51</sup>

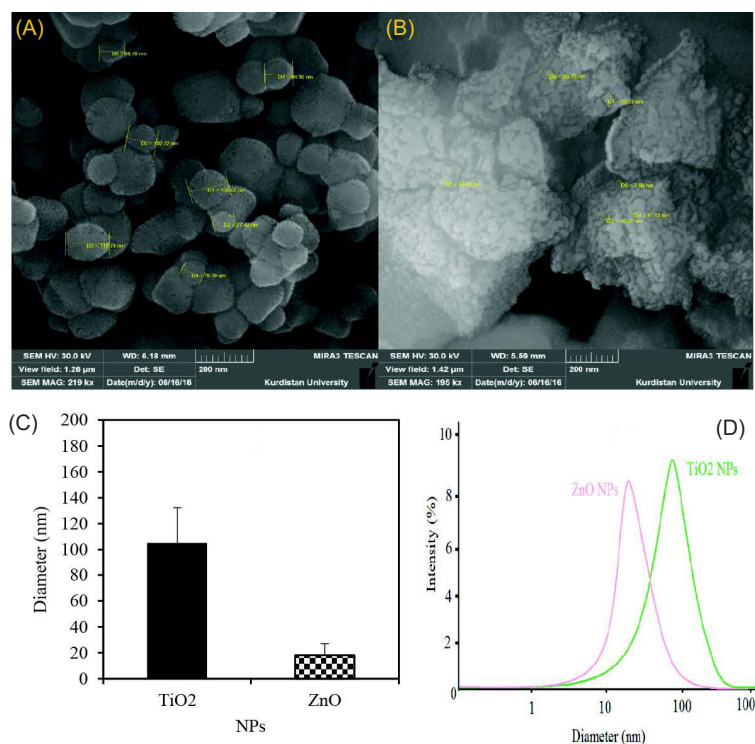


**Fig. 6.** SEM images. The SEM images of  $\text{TiO}_2$  (A), ZnO (B), average particle size (C) and DLS pattern (D) of green synthesized NPs.

Also, it is observed that metal ions can disturb microbial cell walls, break cellular proteins, block cell respiration, and eventually resulted in cell death.<sup>52</sup>

### Discussion

Recently, most antimicrobial agents such as penicillins and cephalosporins with the  $\beta$ -lactams ring are defeated against MDR bacteria. Among the MDR bacteria, methicillin resistant *S. aureus* (MRSA) and *E. coli* with resistance to wide range of antibiotics (tetracycline, aminoglycosides, and chloramphenicol) are prominent pathogenic bacteria which we utilized in the present study. This property of bacteria can be resulted from obtaining of several mechanisms including multidrug efflux pumps, R plasmids, transposons and integrons during evolution phenomenon responded to incorrect using antibiotics.<sup>53,54</sup>

However, production of these antibiotics are increasing annually at an amount of 100 000 tons worldwide.<sup>55</sup> In addition to the higher cost of antibiotics, this phenomenon can also impact on ecosystem.<sup>56</sup> Therefore, application of new strategies without these disadvantages is necessary. In this way, emerging of medicinal nanotechnology by using NPs specifically metal NPs (Ag, Cu, ZnO, and  $\text{TiO}_2$ ) has been a major effect on the approach of antimicrobial agents' synthesis.<sup>57</sup> Many factors including NPs types, cell wall (gram positive and gram negative) and growth rate properties of bacteria, may impact on antibacterial aspects of these NPs.<sup>57</sup> Also, toxicity mechanisms of NPs may be resulted from unique NPs properties such as high surface to volume ratio and radial species production specifically reactive oxygen species (ROS) including hydroxide ( $\text{HO}^\bullet$ ), superoxide ( $\text{O}_2^\bullet$ ) anions and hydrogen peroxide ( $\text{H}_2\text{O}_2$ ).<sup>58</sup> In the case of ZnO NPs, antibacterial effects are due to cell wall damage, increased permeability of the membrane, NPs internalization and ROS production (Fig. 8).<sup>50</sup>

ZnO and  $\text{TiO}_2$  NPs are produced respectively about 31 000-34 000 and 83 500-88 000 metric tons annually worldwide. It can be used in the chemical, physical and green methods for the synthesis of NPs.<sup>59</sup> In this study, the supernatant of *H. elongata* IBRC-M 10214 as the extracellular method was used for the biosynthesis NPs. In this way, organic molecules secreted by the archaeobacteria during growth as well as nutrient media components can contribute to the reduction of  $\text{Zn}^{2+}$  and  $\text{Ti}^{2+}$  ions and NPs biosynthesis.<sup>60</sup> Taguchi method was applied to optimize the setting of the process parameters

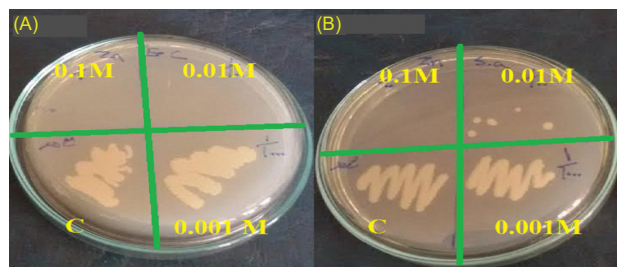


**Fig. 7.** Antibacterial activity: Image showing zone inhibition values of different concentrations of ZnO NPs (0.1, 0.01, 0.001 M of  $\text{ZnCl}_2$ , and control (c)) against two multidrug resistant bacteria *E. coli* ATCC 25922 (A) and *S. aureus* ATCC 43300 (B).

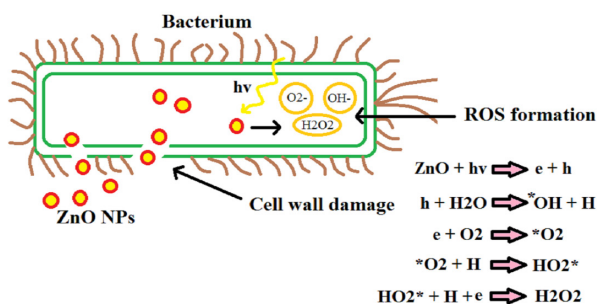


**Fig. 8.** Toxicity mechanisms. Major antibacterial mechanisms of ZnO NPs.

values due to the enhancement of quality properties and identification of the product parameters values under optimal values.<sup>61</sup> Due to analyze the quality properties, Taguchi method applies 3 types of the signal/noise (S/N) ratio. In this study, we used the higher-the-better type of S/N. 3 parameters TiO(OH)<sub>2</sub> concentration, incubation temperature and culturing time for TiO<sub>2</sub> NPs and ZnCl<sub>2</sub> concentration, glucose concentration and incubation temperature for ZnO NPs and their 3 levels were used to design experiment. Results illustrated that TiO(OH)<sub>2</sub> concentrations (44.88%) and culturing time (35.736%) have a respectively higher effect than other parameters in TiO<sub>2</sub> and ZnO NPs biosynthesis.<sup>24,62</sup>

In addition, the FT-IR analysis was performed to indicate the functional groups of bacteria extract that acted as a stabilizer and capping agent in the biosynthesis of ZnO NPs. As shown in Fig. 5, The FT-IR spectra of *H. elongata* IBRC-M 10214 supernatant has demonstrated an absorption broadband at 3387.04 cm<sup>-1</sup> representing O-H stretching of alcohol. The absorption peak is located at 1608.51 cm<sup>-1</sup> are represented N-H bending of amine. Strong absorption peaks at 1146.22 and 1051.11 cm<sup>-1</sup> indicating C-O stretching vibrations of alcohol. Also, absorption peaks at 760.83, 644.31 and 571.95 cm<sup>-1</sup> are confirmed respectively C-Cl stretching and C-Br stretching vibrations of alkyl halide. The absorption peaks in the region of 400-600 cm<sup>-1</sup> are indicated to Zn-O.<sup>30,63</sup>

Antifungal and antibacterial and activities of ZnO NPs were proved respectively against *Aspergillus flavus* (19±1.0 mm) and *P. aeruginosa* (22±1.8 mm).<sup>43</sup> ZnO NPs (19.89±1.43 nm) demonstrated inhibition zone (25 mm) against *B. subtilis*.<sup>64</sup> It was demonstrated that ZnO NPs can result in damaging of *E. coli* membrane by diffusion of the tiny particle ranging from 10 to 80 nm.<sup>65</sup> Zero valent ZnO NPs could interact with intracellular oxygen and cause the damage of the cell membrane by production of oxidative stress.<sup>66</sup> In this case, NPs have revealed higher antibacterial activity with their size decreasing.<sup>67</sup>

## Conclusion

There are many studies about the biosynthesis of NPs by plants, fungi, and bacteria. In this study, we used Taguchi method to obtain optimum conditions in MNPs biosynthesis by *H. elongata* IBRC-M 10214. TiO<sub>2</sub> and ZnO

## Research Highlights

### What is current knowledge?

✓ In the green synthesis as a novel method, bacteria, archaeobacteria, fungi, and plants are used for the production of metal nanoparticles without utilizing any toxic and expensive materials.

### What is new here?

✓ Taguchi method was used to obtain optimum conditions in TiO<sub>2</sub> and ZnO NPs biosynthesis by *H. elongata* IBRC-M 10214.

✓ Antibacterial activity of both biosynthesized ZnO and TiO<sub>2</sub> NPs by *H. elongata* IBRC-M 10214 against *E. coli* ATCC 25922 and *S. aureus* ATCC 43300 was compared.

✓ The biosynthesized ZnO NPs were found to induce greater antibacterial activity than the TiO<sub>2</sub> NPs when used in similar concentration (0.1 M).

NPs with spherical shapes and average diameter sizes of 104.63±27.75 and 18.11±8.93 nm respectively were synthesized through green method. UV-Vis, XRD, FT-IR, and FESEM were applied to the characterization of these 2 types of NPs. Based on this study, a green method is an easy and eco-friendly way for TiO<sub>2</sub> and ZnO NPs synthesis with relative purity of NPs. Also, titanium dioxide and zinc oxide NPs synthesized by *H. elongata* IBRC-M 10214 extracellular and stabilizing of these NPs were possible without using any capping agents which are toxic. Also, ZnO NPs have the antibacterial effect that can be usable in medicinal aspect for fighting against prominent MDR bacteria such as *E. coli* ATCC 25922 and *S. aureus* ATCC 43300. Generally, this study presents simple, low costs, eco-friendly, high productivity with optimum conditions in the fabrication of TiO<sub>2</sub> and ZnO NPs.

### Ethical approval

There is none to be declared.

### Competing interests

No competing interests to be disclosed.

### Acknowledgments

The authors wish to appreciate Razi University for providing necessary facilities to carry out this work.

### Supplementary Materials

Supplementary file 1 contains Tables S1-S7.

### References

1. Tegos G, Stermitz FR, Lomovskaya O, Lewis K. Multidrug pump inhibitors uncover remarkable activity of plant antimicrobials. *Antimicrob Agents Chemother* **2002**; 46: 3133-41. doi: 10.1128/AAC.46.10.3133-3141
2. Gordon YJ, Romanowski EG, McDermott AM. A review of antimicrobial peptides and their therapeutic potential as anti-infective drugs. *Curr Eye Res* **2005**; 30: 505-15. doi: 10.1080/02713680590968637
3. Andersen JL, He G-X, Kakarla P, Kc R, Kumar S, Lakra WS, et al. Multidrug efflux pumps from Enterobacteriaceae, *Vibrio cholerae* and *Staphylococcus aureus* bacterial food pathogens. *Int J Environ Res Public Health* **2015**; 12: 1487-547. doi: 10.3390/ijerph120201487



4. Fisher JF, Meroueh SO, Mobashery S. Bacterial resistance to  $\beta$ -lactam antibiotics: compelling opportunism, compelling opportunity. *Chem Rev* **2005**; 105: 395-424. doi: 10.1021/cr030102i
5. Dizaj SM, Lotfipour F, Barzegar-Jalali M, Zarrintan MH, Adibkia K. Antimicrobial activity of the metals and metal oxide nanoparticles. *Mater Sci Eng C* **2014**; 44: 278-84. doi: 10.1016/j.msec.2014.08.031
6. Alavi M, Karimi N, Safaei M. Application of Various Types of Liposomes in Drug Delivery Systems. *Adv Pharm Bull* **2017**; 7: 3. doi: 10.15171/apb.2017.002
7. Morais MGd, Martins VG, Steffens D, Pranke P, da Costa JAV. Biological applications of nanobiotechnology. *J Nanosci Nanotechnol* **2014**; 14: 1007-17. doi: 10.1166/jnn.2014.8748
8. Zhao Q, Guan J. Love dynamics between science and technology: some evidences in nanoscience and nanotechnology. *Scientometrics* **2013**; 94: 113-32. doi: 10.1007/s11192-012-0785-7
9. Mallakpour S, Madani M. A review of current coupling agents for modification of metal oxide nanoparticles. *Prog Org Coat* **2015**; 86: 194-207. doi: 10.1016/j.porgcoat.2015.05.023
10. Gopiraman M, Deng D, Zhang K-Q, Kai W, Chung I-M, Karvembu R, et al. Utilization of human hair as a synergistic support for Ag, Au, Cu, Ni, and Ru nanoparticles: application in catalysis. *Ind Eng Chem Res* **2017**; 56: 1926-39. doi: 10.1021/ja01867a030
11. Verma J, Lal S, Van Noorden CJF. Nanoparticles for hyperthermic therapy: synthesis strategies and applications in glioblastoma. *Int J Nanomedicine* **2014**; 9:2863-77. doi: 10.2147/IJN.S57501
12. Dhand C, Dwivedi N, Loh XJ, Ying ANJ, Verma NK, Beurman RW, et al. Methods and strategies for the synthesis of diverse nanoparticles and their applications: a comprehensive overview. *RSC Adv* **2015**; 5: 105003-37. doi: 10.1039/C5RA19388E
13. Gentry ST, Fredericks SJ, Krchnavek R. Controlled particle growth of silver sols through the use of hydroquinone as a selective reducing agent. *Langmuir* **2009**; 25: 2613-21. doi: 10.1021/la803680h
14. Zhao P, Feng X, Huang D, Yang G, Astruc D. Basic concepts and recent advances in nitrophenol reduction by gold-and other transition metal nanoparticles. *Coord Chem Rev* **2015**; 287: 114-36. doi: 10.1016/j.ccr.2015.01.002
15. Thakkar KN, Mhatre SS, Parikh RY. Biological synthesis of metallic nanoparticles. *Nanomed Nanotech Biol Med* **2010**; 6: 257-62. doi: 10.1016/j.nano.2009.07.002
16. Ghaseminezhad SM, Hamed S, Shojaosadati SA. Green synthesis of silver nanoparticles by a novel method: a comparative study of their properties. *Carbohydr Polym* **2012**; 89: 467-72. doi: 10.1016/j.carbpol.2012.03.030
17. Iravani S, Zolfaghari B. Green synthesis of silver nanoparticles using *Pinus eldarica* bark extract. *BioMed Res Int* **2013**; 2013: 1-5. doi: 10.1155/2013/639725
18. Srivastava P, Bragança J, Ramanan SR, Kowshik M. Synthesis of silver nanoparticles using haloarchaeal isolate *Halococcus salifodinae* BK3. *Extremophiles* **2013**; 17: 821-31. doi: 10.1007/s00792-013-0563-3. Epub
19. Pereira L, Mehboob F, Stams AJM, Mota MM, Rijnaarts HHM, Alves MM. Metallic nanoparticles: microbial synthesis and unique properties for biotechnological applications, bioavailability and biotransformation. *Crit Rev Biotechnol* **2015**; 35: 114-28. doi: 10.3109/07388551.2013.819484
20. M Joseph M, K George S, T Sreelekha T. Bridging 'Green'with Nanoparticles: Biosynthesis Approaches for Cancer Management and Targeting of Cancer Stem Cells. *Curr Nanosci* **2016**; 12: 47-62. doi: 10.2174/1573413711666150624170401
21. Taran M, Amirkhani H. Strategies of poly(3-hydroxybutyrate) synthesis by *Haloarcula* sp. IRU1 utilizing glucose as a carbon source: Optimization of culture conditions by Taguchi methodology. *Int J Biol Macromol* **2010**; 47: 632-4. doi: 10.1016/j.ijbiomac.2010.08.008
22. Taran M, Azizi E, Taran S, Asadi N. Archaeal Poly(3-hydroxybutyrate) Polymer production from glycerol: Optimization by Taguchi Methodology. *J Polym Environ* **2011**; 19: 750-4. doi:10.1007/s10924-011-0327-z
23. Rodríguez-Sáiz M, Sánchez-Porro C, De La Fuente JL, Mellado E, Barredo JL. Engineering the halophilic bacterium *Halomonas elongata* to produce  $\beta$ -carotene. *Appl Microbiol Biotechnol* **2007**; 77: 637-43. doi: 10.1007/s00253-007-1195-2
24. Saif Hasan S, Singh S, Parikh RY, Dharne MS, Patole MS, Prasad BLV, et al. Bacterial synthesis of copper/copper oxide nanoparticles. *J Nanosci Nanotechnol* **2008**; 8: 3191-6. doi:10.1166/jnn.2008.095
25. Balouiri M, Sadiki M, Ibsouda SK. Methods for in vitro evaluating antimicrobial activity: A review. *J Pharm Biomed Anal* **2016**; 6: 71-9. doi: 10.1016/j.jpba.2015.11.005
26. Buszewski B, Railean-Plugaru V, Pomastowski P, Rafińska K, Szultka-Mlynska M, Golinska P, et al. Antimicrobial activity of biosilver nanoparticles produced by a novel *Streptacidiphilus durhamensis* strain. *J Microbiol Immunol Infect.* **2016**; 16: 30023-8. doi: 10.1016/j.jmii.2016.03.002
27. Paredes D, Ortiz C, Torres R. Synthesis, characterization, and evaluation of the antibacterial effect of Ag nanoparticles against *Escherichia coli* O157:H7 and methicillin-resistant *Staphylococcus aureus* (MRSA). *Int J Nanomedicine* **2014**; 9: 1717-29. doi: 10.2147/IJN.S57156
28. Zhao L, Yu J. Controlled synthesis of highly dispersed TiO<sub>2</sub> nanoparticles using SBA-15 as hard template. *J Colloid Interface Sci* **2006**; 304: 84-91. doi: 10.1016/j.jcis.2006.08.042
29. Liu Y, Sun D, Askari S, Patel J, Macias-Montero M, Mitra S, et al. Enhanced Dispersion of TiO(2) Nanoparticles in a TiO(2)/PEDOT:PSS Hybrid Nanocomposite via Plasma-Liquid Interactions. *Sci Rep* **2015**; 5: 15765. doi: 10.1038/srep15765
30. Elumalai K, Velmurugan S. Green synthesis, characterization and antimicrobial activities of zinc oxide nanoparticles from the leaf extract of *Azadirachta indica* (L.). *Appl Surf Sci* **2015**; 345: 329-36. doi: 10.1016/j.apsusc.2015.03.176
31. Mathew S, kumar Prasad A, Benoy T, Rakesh PP, Hari M, Libish TM, et al. UV-Visible photoluminescence of TiO<sub>2</sub> nanoparticles prepared by hydrothermal method. *J Fluoresc* **2012**; 22: 1563-9. doi: 10.1007/s10895-012-1096-3
32. Khade GV, Suwarnkar MB, Gavade NL, Garadkar KM. Green synthesis of TiO<sub>2</sub> and its photocatalytic activity. *J Mater Sci Mater E* **2015**; 26: 3309-15. doi: 10.1007/s10854-015-2832-7
33. Li Y, Qin Z, Guo H, Yang H, Zhang G, Ji S, et al. Low-temperature synthesis of anatase TiO<sub>2</sub> nanoparticles with tunable surface charges for enhancing photocatalytic activity. *PLoS One* **2014**; 9: e114638. doi: 10.1371/journal.pone.0114638
34. Selvarajan E, Mohanasrinivasan V. Biosynthesis and characterization of ZnO nanoparticles using *Lactobacillus plantarum* VITES07. *Mater Lett* **2013**; 112: 180-2. doi: 10.1016/j.matlet.2013.09.020
35. Shameli K, Ahmad MB, Jazayeri SD, Shabanzadeh P, Sangpour P, Jahangirian H, et al. Investigation of antibacterial properties silver nanoparticles prepared via green method. *Chem Cent J* **2012**; 6: 73-. doi:10.1186/1752-153X-6-73
36. Santhoshkumar T, Rahuman AA, Jayaseelan C, Rajakumar G, Marimuthu S, Kirthi AV, et al. Green synthesis of titanium dioxide nanoparticles using *Psidium guajava* extract and its antibacterial and antioxidant properties. *Asian Pac J Trop Med* **2014**; 7: 968-76. doi: 10.1016/s1995-7645(14)60171-1
37. Zahir AA, Chauhan IS, Bagavan A, Kamaraj C, Elango G, Shankar J, et al. Green Synthesis of Silver and Titanium Dioxide Nanoparticles Using *Euphorbia prostrata* Extract Shows Shift from Apoptosis to G0/G1 Arrest followed by Necrotic Cell Death in *Leishmania donovani*. *Antimicrob Agents Chemother* **2015**; 59: 4782-99. doi: 10.1128/aac.00098-15
38. Jayaseelan C, Rahuman AA, Roopan SM, Kirthi AV, Venkatesan J, Kim SK, et al. Biological approach to synthesize TiO<sub>2</sub> nanoparticles using *Aeromonas hydrophila* and its antibacterial activity. *Spectrochim Acta A Mol Biomol Spectrosc* **2013**; 107: 82-9. doi: 10.1016/j.saa.2012.12.083
39. Fabritz S, Maaß F, Avrutina O, Heiseler T, Steinmann B, Kolmar H. A sensitive method for rapid detection of alkyl halides and dehalogenase activity using a multistep enzyme assay. *AMB Express* **2012**; 2: 51. doi: 10.1186/2191-0855-2-51



40. Luo X, Wang J, Wang C, Zhu S, Li Z, Tang X, et al. Degradation and mineralization of benzohydroxamic acid by synthesized mesoporous La/TiO<sub>2</sub>. *Int J Environ Res Public Health* **2016**; *13*: 997. doi: 10.3390/ijerph13100997
41. Dhandapani P, Maruthamuthu S, Rajagopal G. Bio-mediated synthesis of TiO<sub>2</sub> nanoparticles and its photocatalytic effect on aquatic biofilm. *J Photochem Photobiol* **2012**; *110*: 43-9. doi: 10.1016/j.jphotobiol.2012.03.003
42. Ordenes-Aenishanslins NA, Saona LA, Durán-Toro VM, Monrás JP, Bravo DM, Pérez-Donoso JM. Use of titanium dioxide nanoparticles biosynthesized by *Bacillus mycoides* in quantum dot sensitized solar cells. *Microb Cell Fact* **2014**; *13*: 90. doi: 10.1186/s12934-014-0090-7
43. Jayaseelan C, Rahuman AA, Kirthi AV, Marimuthu S, Santhoshkumar T, Bagavan A, et al. Novel microbial route to synthesize ZnO nanoparticles using *Aeromonas hydrophila* and their activity against pathogenic bacteria and fungi. *Spectrochim Acta Mol Biomol Spectrosc* **2012**; *90*: 78-84. doi: 10.1016/j.saa.2012.01.006
44. Gunalan S, Sivaraj R, Rajendran V. Green synthesized ZnO nanoparticles against bacterial and fungal pathogens. *Prog Nat Sci* **2012**; *22*: 693-700. doi: 10.1016/j.pnsc.2012.11.015
45. Ramesh M, Anbuvannan M, Viruthagiri G. Green synthesis of ZnO nanoparticles using *Solanum nigrum* leaf extract and their antibacterial activity. *Spectrochim Acta A* **2015**; *136*: 864-70. doi: 10.1016/j.saa.2014.09.105
46. Adams CP, Walker KA, Obare SO, Docherty KM. Size-dependent antimicrobial effects of novel palladium nanoparticles. *PLoS ONE* **2014**; *9*: e85981. doi: 10.1371/journal.pone.0085981
47. Azam A, Ahmed AS, Oves M, Khan MS, Habib SS, Memic A. Antimicrobial activity of metal oxide nanoparticles against Gram-positive and Gram-negative bacteria: a comparative study. *Int J Nanomedicine* **2012**; *7*: 6003-9. doi: 10.2147/IJN.S35347
48. Taran M, Rad M, Alavi M. Biological synthesis of copper nanoparticles by using *Halomonas elongata* IBRC-M 10214. *Industria Textila* **2016**; *67*: 351.
49. Taran M, Rad M, Alavi M. Characterization of Ag nanoparticles biosynthesized by *Bacillus* sp. HAI4 in different conditions and their antibacterial effects. *JAPS* **2016**; *6*: 094-9. doi: 10.7324/JAPS.2016.601115
50. Sirelkhatim A, Mahmud S, Seeni A, Kaus NHM, Ann LC, Bakhori SKM, et al. Review on zinc oxide nanoparticles: antibacterial activity and toxicity mechanism. *Nano-Micro Lett* **2015**; *7*: 219-42. doi:10.1007/s40820-015-0040-x
51. Vidic J, Stankic S, Haque F, Ciric D, Le Goffic R, Vidy A, et al. Selective antibacterial effects of mixed ZnMgO nanoparticles. *J Nanopart Res* **2013**; *15*: 1595. doi:10.1007/s11051-013-1595-4
52. Hsueh Y-H, Lin K-S, Ke W-J, Hsieh C-T, Chiang C-L, Tzou D-Y, et al. The antimicrobial properties of silver nanoparticles in *Bacillus subtilis* are mediated by released Ag(+) Ions. *PLoS One* **2015**; *10*: e0144306. doi: 10.1371/journal.pone.0144306
53. Magiorakos AP, Srinivasan A, Carey RB, Carmeli Y, Falagas ME, Giske CG, et al. Multidrug-resistant, extensively drug-resistant and pandrug-resistant bacteria: an international expert proposal for interim standard definitions for acquired resistance. *Clin Microbiol Infect* **2012**; *18*: 268-81. doi: 10.1111/j.1469-0691.2011.03570.x
54. Mahmoudi M, Zhao M, Matsuura Y, Laurent S, Yang PC, Bernstein D, et al. Infection-resistant MRI-visible scaffolds for tissue engineering applications. *Bioimpacts* **2016**; *6*: 111. doi:10.15171/bi.2016.16
55. Nikaido H. Multidrug resistance in bacteria. *Annu Rev Biochem* **2009**; *78*: 119-46. doi: 10.1146/annurev.biochem.78.082907.145923
56. Costanzo SD, Murby J, Bates J. Ecosystem response to antibiotics entering the aquatic environment. *Marine Poll Bull* **2005**; *51*: 218-23. doi: 10.1016/j.marpolbul.2004.10.038
57. Hajipour MJ, Fromm KM, Ashkarran AA, de Aberasturi DJ, de Larramendi IR, Rojo T, et al. Antibacterial properties of nanoparticles. *Trends Biotechnol* **2012**; *30*: 499-511. doi: 10.1016/j.tibtech.2012.06.004
58. Le Ouay B, Stellacci F. Antibacterial activity of silver nanoparticles: a surface science insight. *Nano Today* **2015**; *10*: 339-54. doi: 10.1016/j.nantod.2015.04.002
59. Peralta-Videa JR, Huang Y, Parsons JG, Zhao L, Lopez-Moreno L, Hernandez-Viezcas JA, et al. Plant-based green synthesis of metallic nanoparticles: scientific curiosity or a realistic alternative to chemical synthesis? *Nano Environ Eng* **2016**; *1*: 4. doi:10.1007/s41204-016-0004-5
60. Singh R, Shedbalkar UU, Wadhvani SA, Chopade BA. Bacteriogenic silver nanoparticles: synthesis, mechanism, and applications. *Appl Microbiol Biotechnol* **2015**; *99*: 4579-93. doi:10.1007/s00253-015-6622-1
61. Yang WHp, Tarnq YS. Design optimization of cutting parameters for turning operations based on the Taguchi method. *J Mater Process Technol* **1998**; *84*: 122-9. doi: 10.1016/s0924-0136(98)00079-x
62. Zhu H-t, Lin Y-s, Yin Y-s. A novel one-step chemical method for preparation of copper nanofluids. *J Colloid Interface Sci* **2004**; *277*: 100-3. doi: 10.1016/j.jcis.2004.04.026
63. Sangeetha G, Rajeshwari S, Venkatesh R. Green synthesis of zinc oxide nanoparticles by aloe barbadensis miller leaf extract: Structure and optical properties. *Mater Res Bull* **2011**; *46*: 2560-6. doi: 10.1016/j.materresbull.2011.07.046
64. Hsueh Y-H, Ke W-J, Hsieh C-T, Lin K-S, Tzou D-Y, Chiang C-L. ZnO nanoparticles affect *Bacillus subtilis* cell growth and biofilm formation. *PLoS ONE* **2015**; *10*: e0128457. doi: 10.1371/journal.pone.0128457
65. Das S, Sinha S, Das B, Jayabalan R, Suar M, Mishra A, et al. Disinfection of multidrug-resistant *Escherichia coli* by solar-photocatalysis using Fe-doped ZnO nanoparticles. *Sci Rep* **2017**; *7*: 104. doi:10.1038/s41598-017-00173-0
66. Manke A, Wang L, Rojanasakul Y. Mechanisms of nanoparticle-induced oxidative stress and toxicity. *Bio Med Res Int* **2013**; *2013*: 942916. doi:10.1155/2013/942916
67. Bondarenko O, Ivask A, Käkinen A, Kurvet I, Kahru A. Particle-cell contact enhances antibacterial activity of silver nanoparticles. *PLoS One* **2013**; *8*: e64060. doi:10.1371/journal.pone.0064060